Acta Geochim (2019) 38(5):613–626
https://doi.org/10.1007/s11631-019-00359-5

ORIGINAL ARTICLE

Influence of the biological carbon pump effect on the sources and deposition of organic matter in Fuxian Lake, a deep oligotrophic lake in southwest China

Haibo He[1,2] · Zaihua Liu[1,3] · Chongying Chen[1] · Yu Wei[1,2] · Qian Bao[1,2] · Hailong Sun[1] · Yundi Hu[1,2] · Hao Yan[1]

Received: 25 March 2019 / Revised: 28 April 2019 / Accepted: 4 June 2019 / Published online: 26 June 2019

Abstract Biological carbon pumping (BCP) is a key process in which dissolved inorganic carbon in terrestrial aquatic ecosystems is utilized by aquatic autotrophs for photosynthesis and transformed into autochthonous organic matter (AOC). However, the mechanisms underlying BCP and the amount of generated AOC deposited effectively, are still poorly understood. Therefore, we conducted a systematic study combining modern hydrochemical monitoring and a sediment trap experiment in Fuxian Lake (Yunnan, SW China), the second-deepest plateau, oligotrophic freshwater lake in China. Temperature, pH, EC (electrical conductivity), DO (dissolved O_2), [HCO_3^-], [Ca^{2+}], SI_c, partial CO_2 (pCO_2) pressure, and carbon isotopic compositions of HCO_3^- ($\delta^{13}C_{DIC}$) in water from Fuxian Lake all displayed distinct seasonal and vertical variations. This was especially apparent in an inverse correlation between pCO_2 and DO, indicating that variations of hydrochemistry in the lake water were mainly controlled by the metabolism of the aquatic phototrophs. Furthermore, the lowest C/N ratios and highest $\delta^{13}C_{org}$ were recorded in the trap sediments. Analyses of the C/N ratio demonstrated that the proportions of AOC ranged from 30% to 100% of all OC, indicating that AOC was an important contributor to sedimentary organic matter (OC). It was calculated that the AOC flux in Fuxian Lake was 20.43 t C km^{-2} in 2017. Therefore, AOC produced by carbonate weathering and aquatic photosynthesis could potentially be a significant carbon sink and may have an important contribution to solving the lack of carbon sinks in the global carbon cycle.

Keywords Carbonate weathering · Hydrochemical variation · Biological carbon pump effect · Sediment trap · Autochthonous organic carbon · Carbon sink

1 Introduction

Anthropogenic emissions of CO_2 from burning fossil fuels, industry, and land use have increased atmospheric CO_2 concentration to 409 ppm in 2018 since the beginning of the industrial period in the late 18th century (i.e., over the Anthropocene). Many mass balance calculations for CO_2, however, have revealed an imbalance in the atmospheric CO_2 budget (Broecker et al. 1979; Ciais et al. 2013; Melnikov and O'Neill 2006; Schindler 1999; Sundquist 1993). Identifying missing carbon sinks is, therefore, a top priority in the science of global climate change.

Cole et al. (1994) found that globally, lakes influence the terrestrial carbon budget significantly through the efflux of CO_2 to the atmosphere, indicating that they are carbon sources rather than sinks. However, when sediment accumulation is taken into account, research has shown that a large quantity of carbon from terrestrial sources is buried in aquatic sediments (Cole et al. 2007; Xiao 2017). Other studies (Liu et al. 2010, 2011, 2018) have suggested that the weathering of carbonate minerals, often coupled with aquatic photosynthesis (the biological carbon pump effect or "BCP"), may be a carbon sink and an important

✉ Zaihua Liu
liuzaihua@vip.gyig.ac.cn

[1] State Key Laboratory of Environmental Geochemistry, Institute of Geochemistry, CAS, Guiyang 550081, China

[2] University of Chinese Academy of Sciences, Beijing 100049, China

[3] CAS Center for Excellence in Quaternary Science and Global Change, Guiyang 550081, China

contributor to the missing global carbon. Rapid carbonate weathering (Liu and Dreybrod 1997) provides abundant dissolved inorganic carbon (DIC), and aquatic photosynthesis takes up the latter as its carbon source when the BCP effect occurs in aquatic ecosystems. This means that the autochthonous organic carbon (OC) in organic sediments, especially from karst basins, is a significant sink for anthropogenic CO_2. Therefore, the carbon sink resulting from combining carbonate weathering with aquatic photosynthesis (CCW) might be very important for controlling climate change at any time scale (Liu et al. 2011, 2018).

Lacustrine OC can reflect a complex mixture of different sources, including autochthonous and allochthonous OC. When compared to autochthonous OC, allochthonous OC represents terrigenous sources such as vascular plant tissue and detritus from marshes and upland sources (O'Reilly et al. 2014). Some studies show that lakes can bury considerable amounts of OC in sediments that include inputs from both aquatic primary production and terrestrially fixed organic matter (Galy et al. 2011; Waterson and Canuel 2008; Huang et al. 2017). However, the relative contributions of autochthonous and allochthonous sources, which regulates OC burial in sediment, and the mechanisms underlying these, remain to be determined. Traditional geochemical methods (C/N, $\delta^{13}C_{org}$) used to study organic matter can be ideal tools with which to determine the sources of organic matter in sediments (Meyers and Ishiwatari 1993; Ramaswamy et al. 2008; Tue et al. 2011). $\delta^{13}C_{org}$ has been used as a proxy indicator of productivity (e.g., Hollander and McKenzie 1991; Brenner et al. 1999), whereas C/N ratio values indicate the relative contribution of allochthonous versus autochthonous organic matter in lake sediment (Meyers and Ishiwatari 1993; Meyers 1997, 2003).

In view of this, a systematic study of hydrochemical monitoring and trap sediments was conducted in Fuxian Lake, the second-deepest plateau oligotrophic freshwater lake in southwest China. Here we address the following questions: (1) Are hydrogeochemical changes affected by the process of BCP? (2) Is the sedimentary OC in Fuxian Lake mainly derived from autochthonous or allochthonous sources? (3) How much is the sedimentary flux of organic carbon generated by the BCP effect in Fuxian Lake? (4) Do anthropogenic activities and climatic change affect sedimentary fluxes?

2 Field setting

Fuxian Lake (24°17′–24°37′N, 102°49′–102°57′E) is an oligotrophic lake located in central Yunnan Province, Southwest China (Fig. 1). The catchment area is 675 km^2, while the lake has a surface area of 212 km^2 and a maximum depth of 158 m. It has an average altitude of 1723 m above sea level (asl). The lake basin is wide and deep in the north and narrow and comparatively shallow in the south, with one significant inflowing stream (Liangwang River) to the north, numerous small stream- and spring-fed inflows (e.g., Luchong Spring), and a single outlet (the Haikou River). It has an estimated water retention time of 167 years (Wang and Dou 1998). Present climatic conditions in this region are typically dominated by the Indian Summer Monsoon and experience seasonality. The region is characterized by an average temperature of 15.6 °C, with 951 mm of annual average precipitation, and 83% of the total annual precipitation occurs between May and October (http://www.yncj.gov.cn/).

3 Methods

3.1 Field monitoring

Physical and chemical variables were monitored in the water column and samples were collected quarterly from the northern, central, and southern regions of the lake throughout 2017. Temperature (T), pH, electrical conductivity (EC), and dissolved oxygen (DO) profiles were obtained at 10 m intervals from the surface (0.5 m) to the bottom (110 m) of the water column using a multiparameter water quality probe (WTW; Wissenschaftlich-Technische-Werkstaetten Technology Multiline 350i). The meters were calibrated prior to deployment using standards for pH (4, 7, and 10), EC (1412 μs cm^{-1}) and DO (0% and 100%). The measuring accuracy of the pH, T, DO, and EC was 0.01, 0.01 °C, 0.01 mg L^{-1}, and 0.01 μs cm^{-1}, respectively. The major spring (the Luchong) and river (the Liangwang) located along the western and northern shore, respectively, (Fig. 1) were also sampled.

3.2 Water sampling and analysis

Two sets of water samples were filtered in the field using 0.45 μm Millipore nitrocellulose filters and 20 ml of these samples were stored for measuring major cation and anion contents. Cation samples were acidified with concentrated ultra-pure HNO_3 to pH < 2 to prevent complexation and precipitation. Both anionic and cationic samples were refridgerated at 4 °C.

Anions (Cl^-, SO_4^{2-}, and NO_3^-) were measured by ICS-90 ion chromatograph, and major cations (K^+, Na^+, Ca^{2+}, and M g^{2+}) were determined with an inductively coupled plasma optical emission spectrometer (ICP-OES). Reagent and procedural blanks were determined in parallel to the sample treatment. The experimental detection resolution of these ions was 0.01 mg L^{-1}. In addition, alkalinity (chiefly

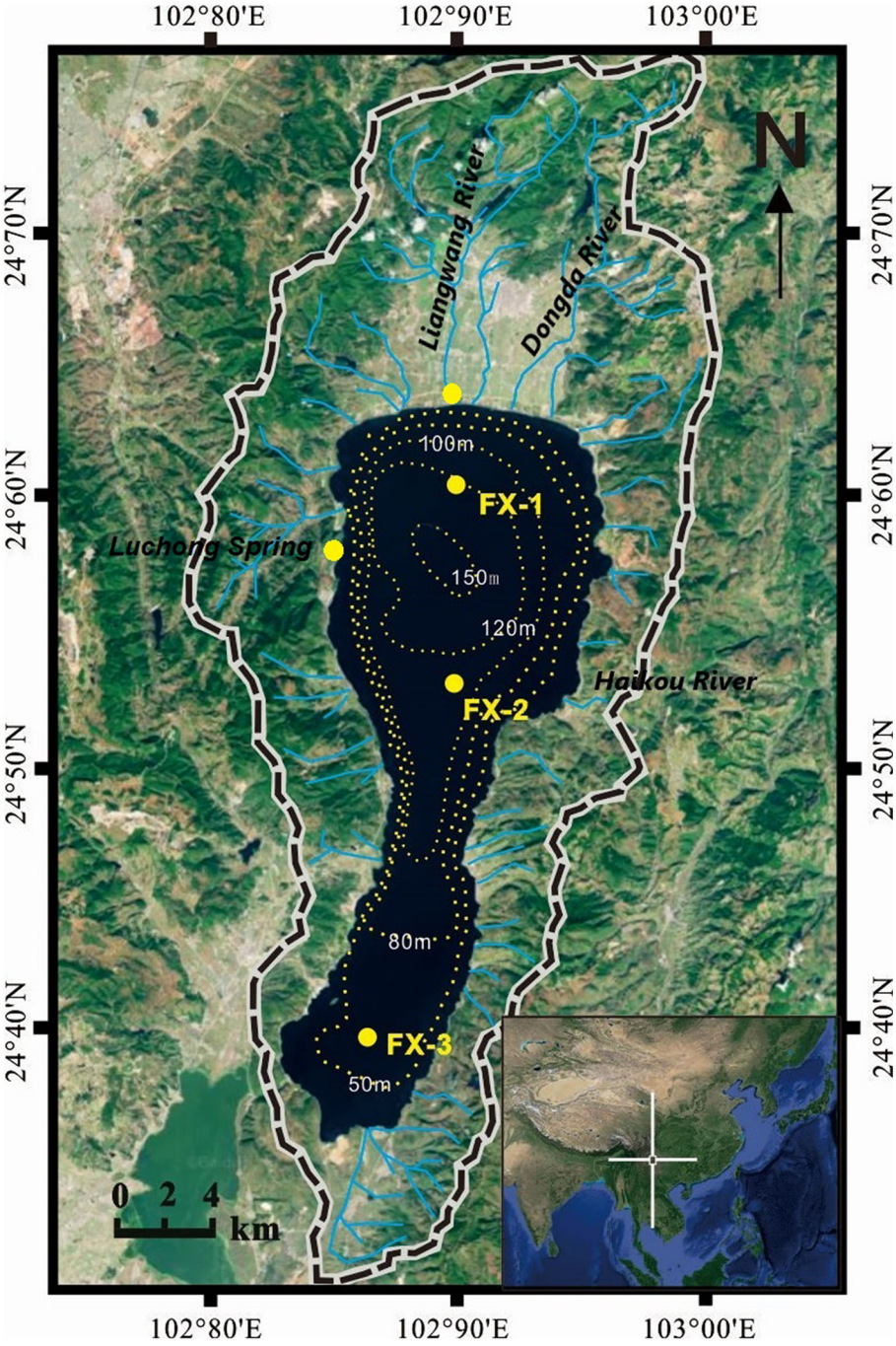

Fig. 1 Schematic map of the Fuxian Lake basin with sampling points indicated by filled circles (Luchong Spring, Liangwang River and Fuxian Lake). FX-1, FX-2 and FX-3 are sampling sites representing the northern, central and southern sectors of the Lake, respectively. The basin boundary (black dashed line) and lake depth contours (dotted lines) are from Liu et al. (2008)

as HCO_3^-) were in situ titrated by an Aquamerck alkalinity test kit supplied by Merck (Germany), with an estimated accuracy of 0.05 mmol L^{-1}. In addition, ion concentrations were used to calculate the CO_2 partial pressure (pCO_2) and calcite saturation index (SI_c) from a geochemical model with pH, temperature, and seven major ions concentrations using the PHREEQC3 model (Parkhurst and Appelo 1999).

The remaining water samples (60 ml) were filtered by pressure filtration through 0.45 μm cellulose acetate filters and stored in previously acid-washed HDPE bottles with air-tight caps and no air bubbles or headspace for subsequent measurement of $\delta^{13}C_{DIC}$. One drop of saturated $HgCl_2$ solution was added to each sample to prevent microbial activity, and all samples were stored in a refrigerator at 4 °C until analyzed by MAT-252 mass spectrometry.

3.3 Sediment sampling and analyses

Settling particulate material was collected quarterly in three sediment traps deployed throughout 2017. The traps were simple open-topped cylindrical polyethylene tubes

with an aspect ratio of 7:1 (105 cm in length, with an inner diameter of 15 cm). Material was obtained from depths of 40, 80, and 110 m in the center of the lake (depth of water about 120 m at site FX-2, Fig. 1). After recovery of the sediment traps, the material collected was transferred into plastic containers in the field and stored at 4 °C prior to sub-sampling, then freeze-dried. The homogeneous dry material of the sediment traps was weighed, and mass accumulation rates k (g m^{-2} day^{-1}) of dry material were calculated using:

$$k = \frac{m}{a * t} \quad (1)$$

where m (g) is the dry mass collected, a (m^2) is the open trap area, and t (day) is the time interval of exposure.

3.4 Measurement of organic carbon, inorganic carbon, and TOC/TN

Total carbon (TC) was measured using an elemental analyzer (Elementar-vario MACRO cube), which was calibrated using sediment standard materials (B2150 and AR2026) to an analytical precision better than 0.2%. Total organic carbon (TOC), total nitrogen (TN) content, and TOC/TN (atomic) ratios were determined for the sediments following acid treatment with 1.5 mol/L HCl for 24 h to remove inorganic carbon. The carbonate-free samples were triple-rinsed with distilled water to remove acid residues, dried at 60 °C for 48 h, and measured using the MACRO analyzer. The total inorganic carbon (TIC) content was then calculated as the difference between TC and TOC.

The rates of accumulation of organic carbon (OCAR) and inorganic carbon (ICAR) (g C m^{-2} day^{-1}) were estimated using the following formula:

$$\text{OCAR (or ICAR)} = k * C \quad (2)$$

where k (g m^{-2} day^{-1}) is mass accumulation rates of dry material and C is the content of organic carbon (or inorganic carbon) (mg g^{-1}).

3.5 Measurement of stable carbon isotope ratios

The stable carbon isotope ratios ($\delta^{13}C$) of organic carbon and inorganic carbon in the samples were determined using a MAT-252/253 mass spectrometer. Isotopic composition is reported relative to the international Vienna Peedee Belemnite (VPDB) standard. Analytical precision was typically better than ± 0.03‰ based on replicate measurements of an internal laboratory standard (Sun et al. 2011). All isotopic compositions of samples mentioned in this paper are expressed as "δ" values, representing deviations in per mil (‰) from the standard:

$$\delta^{13}C_{sample} = \left(R_{sample}/R_{standard} - 1\right) \times 1000 \quad (3)$$

where R is the $^{13}C/^{12}C$ ratio of the sample or standard.

3.6 Calculation of OCAR from autochthonous and allochthonous sources

The values of the C/N ratios indicate the relative contribution of allochthonous versus autochthonous organic matter to lake sediments (Meyers and Ishiwatari 1993; Meyers 1997, 2003). Autochthonous and allochthonous sources of OC in trap sediments can be calculated from the following:

$$\frac{C_{auto}}{C_{allo}} = \frac{C/N_{auto}}{C/N_{allo}} \cdot \frac{C/N_i - C/N_{allo}}{C/N_{auto} - C/N_m} \quad (4)$$

where C_{auto} and C_{allo} are the proportion of autochthonous and allochthonous OC, respectively, C/N_i is the C/N ratio of a given sample, C/N_{auto} is the C/N ratio of the autochthonous endmember (7.02), and C/N_{allo} is the C/N ratio of the allochthonous endmember (12.71).

The organic carbon accumulation rates from autochthonous and allochthonous OC can then be calculated by:

$$OCAR_{auto}(\text{or } OCAR_{allo}) = OCAR \times C_{auto}(\text{or } C_{allo}) \quad (5)$$

where $OCAR_{auto}$ (g C m^{-2} day^{-1}) and $OCAR_{allo}$ (g C m^{-2} day^{-1}) are the organic carbon accumulation rates from autochthonous and allochthonous OC, respectively.

4 Results

4.1 Spatial–temporal physicochemical variations in river, spring, and Fuxian Lake water

Temporal and spatial variations in water chemistry and carbon isotopes in Luchong Spring, Liangwang River, and surface water from Fuxian Lake are summarized in Tables 1 and 2. All parameters in the spring and river water showed little seasonal variation, with the coefficients of variation (CV) generally being < 1% (Table 1, Fig. 2). In addition, the spring and river water had a lower pH, DO, SI_c, and a higher [Ca^{2+}] and pCO_2 than the surface water from Fuxian Lake.

The vertical profiles of lake water temperature displayed thermal stratification and the thermocline was located between 20 and 50 m from April to October 2017. In contrast, it was well mixed between 0 and 50 m in January 2017 (Fig. 3). The hydrochemical facies of the water column under different seasons are shown in a Piper diagram in Fig. 4. The major cations were Ca^{2+} and Mg^{2+}, and the

Table 1 Statistics on the seasonal variations of physicochemical parameters in the spring and river

Site	T (°C)	pH	EC (μs cm^{-1})	DO (mg L^{-1})	[Ca^{2+}] (mg L^{-1})	[HCO_3^-] (mg L^{-1})	SI_c	pCO_2 (Pa)	$\delta^{13}C_{DIC}$ (‰)
Spring	22.8–27.2[a]	7.5–7.8	244.0–277.7	5.7–6.5	34.7–44.5	170.8–183.0	0.0–0.2	314.8–511.7	− 10.1–8.2
	(24.9)[b] [6.2][c]	(7.7) [1.2]	(260.6) [5.2]	(6.2) [4.9]	(39.9) [9.1]	(176.9) [2.4]	(0.1) [78.5]	(378.4) [20.6]	(− 9.1) [− 8.5]
River	14.0–18.6	8.1–8.5	301.3–430.0	6.3–7.5	36.9–64.7	170.8–207.4	0.3–1.0	45.7–120.2	− 10.4–8.0
	(17.0) [10.5]	(8.3) [2.0]	(363.0) [12.6]	(6.8) [7.4]	(51.8) [22.2]	(184.5) [7.5]	(0.7) [36.4]	(87.0) [32.1]	(− 9.6) [− 9.9]

[a]Minimum–maximum

[b]Mean values

[c]CV or variation coefficients = (standard deviation/mean) %

major anion was HCO_3^-. The hydrochemical type was of simple HCO_3^-–Ca–Mg, indicating typical karst water.

The vertical variations in pH, DO, and SI_c in the water column were similar to that of T during thermal stratification in April, July, and October, indicating that the vertical water exchange was effectively limited by thermal stratification. These values were much higher in the epilimnion than in deep water. In contrast, the EC, [Ca^{2+}], [HCO_3^-], and pCO_2 in the epilimnion were lower than those in deep water during both summer stratification and winter mixing (Fig. 3).

The $\delta^{13}C_{DIC}$ variations in spring, river, and lake water in the 4 months are presented in Fig. 5 and Tables 1 and 2. $\delta^{13}C_{DIC}$ values of spring and river waters exhibited no discernible seasonal variation, with the CV values of 0.1 for both spring and river waters. However, the $\delta^{13}C_{DIC}$ variations of surface waters varied seasonally, being most negative in winter. Figure 5 shows the depth profiles of $\delta^{13}C_{DIC}$ in Fuxian Lake obtained between January and October 2017. The lake was homogeneous with respect to $\delta^{13}C_{DIC}$ in the epilimnion between 0 m and 50 m during the winter mixing period. $\delta^{13}C_{DIC}$ values decreased in the hypolimnetic waters.

4.2 Contents, accumulation rates and carbon isotope ratios of organic and inorganic carbon in trap sediments

Throughout the year (January 2017–January 2018) of sediment trapping in Fuxian Lake, the collected material revealed distinct changes (Table 3). Total accumulation rates (total AR) derived from sediment traps were substantially higher during summer and fall (1.00–2.95 g C m^{-2} day^{-1}) than during spring and winter (0.44–0.70 g C m^{-2} day^{-1}).

There were higher values (92.21–107.78 mg g^{-1}) of TOC in the winter and spring, while higher TIC (63.54–80.83 mg g^{-1}) occurred in the summer and fall. There were positive correlations between inorganic carbon accumulation rates (ICAR) and organic carbon accumulation rates (OCAR), with both reaching their highest values in summer and fall (ICAR: 0.07–0.24 g C m^{-2} day^{-1}; OCAR: 0.08–0.13 g C m^{-2} day^{-1}) (Table 3). The C/N ratio is a frequently-used index feature of sediments, which was essentially lower than 10 in the current study. There were positive correlations between $\delta^{13}C_{org}$ (− 20.88 to − 25.37 ‰) and $\delta^{13}C_{carb}$ (− 0.35–0.007 ‰), with higher values in summer and fall (Table 3).

The calculated average contributions of autochthonous OC in these trap sediments ranged from 30 to 100%. The $OCAR_{auto}$ ranged from 0.02 to 0.13 g C m^{-2} day^{-1}, with an average of 0.04 g C m^{-2} day^{-1} (Table 4).

5 Discussion

5.1 Mechanisms for the temporal-spatial variations of water chemistry and carbon isotope in Fuxian Lake: role of biological carbon pump effect

Fuxian Lake has a large open water surface area and volume and a small catchment area, with a long water retention time of 167 years (Wang and Dou 1998). It receives water from more than 20 small rivers, indicating that the body of the lake has a strong buffer effect on inputs from allochthonous sources. In contrast, Liangwang River, the largest river entering the lake, showed seasonal fluctuations in the physicochemical parameters which are consistent with values in the surface water of Fuxian Lake during the sampling year (Fig. 2). However, these data cannot explain variations in the depth profiles from Fuxian Lake. All parameters in Luchong Spring showed an opposite trend to that of the surface water of Fuxian Lake (Fig. 2). Therefore, the physical and chemical parameters in the depth profiles of Fuxian Lake were not controlled by river and spring input.

Some lakes are supersaturated with CO_2 and consequently emit CO_2 to the atmosphere (Sobek et al. 2005;

Table 2 Statistics on the seasonal variations of physicochemical parameters at different depths in Fuxian Lake

Sample no.	Depth (m)	T (°C)	pH	EC (μs cm^{-1})	DO (mg L^{-1})	[Ca^{2+}] (mg L^{-1})	[HCO_3^-] (mg L^{-1})	SI_c	pCO_2 (Pa)	$\delta^{13}C_{DIC}$ (‰)
FX-1-1	0	15.4–22.4[a]	8.5–9.1	286.8–318.0	7.7–9.0	20.1–26.2	176.9–207.4	0.6–1.1	11.8–45.7	− 1.2–2.1
		(18.8)[b] [15.3][c]	(8.8) [2.3]	(303.3) [4.4]	(8.5) [5.6]	(23.2) [10.4]	(187.6) [6.2]	(0.9) [20.0]	(26.1) [0.5]	(0.4) [314.8]
FX-1-2	10	15.4–21.8	8.5–9.1	286.7–318.0	7.8–8.8	19.9–26.1	170.8–189.1	0.6–1.1	11.8–48.0	− 1.2–1.6
		(18.6) [14.5]	(8.8) [2.5]	(303.5) [4.5]	(8.4) [4.5]	(23.2) [10.8]	(180.7) [3.7]	(0.8) [21.5]	(27.0) [0.5]	(0.2) [575.2]
FX-1-3	20	15.3–20.9	8.5–8.9	287.5–318.0	7.6–8.2	19.8–26.2	164.7–201.3	0.6–0.9	16.9–45.7	− 1.2–1.6
		(18.3) [13.5]	(8.7) [1.7]	(306.0) [4.0]	(8.0) [8.8]	(23.4) [10.1]	(182.0) [7.2]	(0.8) [13.7]	(30.7) [0.4]	(0.2) [481.4]
FX-1-4	30	15.3–20.3	8.5–8.8	290.0–318.0	7.4–8.2	19.9–26.2	170.8–189.1	0.6–0.8	20.4–45.8	− 1.3–1.5
		(16.7) [12.3]	(8.7) [1.7]	(307.4) [3.7]	(7.6) [9.0]	(23.6) [10.2]	(177.9) [4.3]	(0.7) [15.2]	(33.9) [0.3]	(0.2) [483.6]
FX-1-5	40	14.4–18.9	8.4–8.7	301.7–318.0	5.4–7.8	22.1–26.3	183.0–195.2	0.5–0.7	27.8–61.9	− 1.2–0.9
		(15.9) [11.0]	(8.6) [1.2]	(311.0) [2.3]	(6.4) [15.1]	(24.1) [6.7]	(187.6) [2.7]	(0.6) [10.5]	(43.7) [0.3]	(− 0.3) [− 305.0]
FX-1-6	50	14.5–16.3	8.4–8.7	298.3–318.0	5.5–7.8	22.0–26.3	176.9–195.2	0.5–0.7	26.6–66.5	− 1.2–1.2
		(15.2) [4.6]	(8.6) [1.6]	(310.0) [2.7]	(6.4) [13.5]	(24.1) [7.1]	(187.6) [4.2]	(0.6) [14.0]	(43.2) [0.4]	(− 0.2) [− 601.2]
FX-1-7	60	14.4–15.3	8.3–8.8	299.7–322.0	4.7–6.3	21.7–26.3	179.0–195.2	0.4–0.8	22.4–78.3	− 1.7–1.1
		(14.8) [2.2]	(8.6) [2.1]	(311.0) [3.0]	(5.7) [10.1]	(24.0) [7.4]	(188.1) [3.8]	(0.6) [20.4]	(45.4) [0.5]	(− 0.3) [− 470.9]
FX-1-8	70	14.3–15.0	8.3–8.8	300.3–322.0	4.8–6.0	21.7–26.3	183.0–195.2	0.4–0.7	25.1–75.2	− 1.7–1.8
		(14.5) [2.0]	(8.5) [2.0]	(311.5) [3.0]	(5.6) [9.0]	(24.0) [7.5]	(186.0) [2.8]	(0.6) [21.9]	(47.5) [0.4]	(0.0) [3042.9]
FX-1-9	80	13.9–14.8	8.3–8.7	304.3–323.0	4.3–5.9	22.4–26.3	176.9–201.3	0.4–0.7	26.3–81.3	− 1.8–1.6
		(14.4) [2.6]	(8.5) [2.0]	(313.1) [2.7]	(5.3) [11.4]	(24.3) [6.6]	(187.6) [4.8]	(0.5) [22.4]	(53.5) [0.4]	(− 0.2) [− 624.1]
FX-1-10	90	14.3–14.7	8.3–8.8	302.3–321.0	4.8–5.6	22.4–26.4	176.9–195.2	0.4–0.8	23.1–76.7	−1.5–1.7
		(14.5) [1.3]	(8.5) [2.3]	(311.8) [2.8]	(5.3) [5.8]	(24.2) [6.7]	(184.0) [3.7]	(0.5) [26.5]	(51.3) [0.4]	(− 0.1) [− 1436.6]
FX-1-11	100	13.7–14.5	8.3–8.7	303.3–322.0	4.6–5.6	22.1–26.4	176.9–195.2	0.4–0.7	31.2–75.9	− 1.7–1.2
		(14.2) [2.3]	(8.5) [1.9]	(313.1) [2.6]	(5.3) [7.5]	(24.3) [6.6]	(184.5) [3.6]	(0.5) [23.6]	(53.6) [0.4]	(− 0.2) [− 528.7]
FX-1-12	110	14.1–14.6	8.3–8.7	303.3–322.0	4.2–5.5	22.2–26.5	183.0–195.2	0.3–0.7	26.4–84.1	− 1.6–1.8
		(14.4) [1.3]	(8.5) [2.2]	(313.3) [2.8]	(5.1) [10.1]	(24.1) [6.9]	(186.0) [2.8]	(0.5) [26.8]	(53.9) [0.4]	(− 0.1) [− 2126.6]
FX-2-1	0	15.4–22.9	8.5–8.9	287.1–318.0	7.7–9.0	19.7–25.3	183.0–201.3	0.6–0.9	17.0–54.1	− 1.1–3.1
		(19.0) [16.1]	(8.8) [1.9]	(304.5) [4.2]	(8.4) [5.3]	(22.9) [9.8]	(190.1) [3.6]	(0.8) [16.2]	(29.8) [0.5]	(0.8) [206.3]
FX-2-2	10	15.2–22.5	8.5–8.9	287.4–318.0	7.8–8.6	19.5–25.3	183.0–195.2	0.6–0.9	18.3–49.9	− 1.3–2.9
		(18.6) [16.2]	(8.8) [1.9]	(305.2) [4.1]	(8.0) [6.0]	(23.0) [10.2]	(186.0) [2.8]	(0.8) [16.5]	(29.1) [0.4]	(0.5) [322.5]
FX-2-3	20	15.1–21.1	8.5–8.9	287.5–317.0	6.7–8.3	20.0–25.1	176.9–201.3	0.5–0.9	18.6–51.5	− 1.2–1.6
		(18.2) [14.2]	(8.7) [1.8]	(306.2) [3.9]	(7.6) [7.9]	(23.2) [8.9]	(186.0) [4.9]	(0.8) [17.6]	(32.7) [0.4]	(0.2) [508.9]
FX-2-4	30	15.1–20.3	8.4–8.8	290.6–317.0	6.0–7.7	20.1–25.6	176.9–201.3	0.5–09	22.7–61.4	− 1.2–2.1
		(17.7) [13.3]	(8.6) [1.6]	(308.0) [3.6]	(7.1) [9.6]	(23.3) [9.2]	(187.1) [5.0]	(0.7) [16.0]	(41.0) [0.3]	(0.3) [526.3]
FX-2-5	40	14.8–18.5	8.5–8.6	302.6–318.0	5.2–8.2	22.0–25.5	170.8–189.1	0.6–0.8	42.6–49.0	− 1.3–1.4
		(15.9) [9.8]	(8.5) [0.2]	(311.2) [2.1]	(6.8) [17.5]	(24.0) [6.2]	(183.0) [4.1]	(0.6) [5.4]	(44.6) [0.1]	(− 0.1) [− 1880.4]

Table 2 continued

Sample no.	Depth (m)	T (°C)	pH	EC (μs cm^{-1})	DO (mg L^{-1})	[Ca^{2+}] (mg L^{-1})	[HCO_3^-] (mg L^{-1})	SI_c	pCO_2 (Pa)	$\delta^{13}C_{DIC}$ (‰)
FX-2-6	50	14.5–16.5	8.5–8.6	298.9–318.0	5.3–7.7	22.5–25.1	183.0–207.4	0.6–0.6	38.2–50.1	− 1.3–2.8
		(15.2) [5.4]	(8.5) [0.4]	(311.1) [2.6]	(6.6) [13.4]	(24.0) [4.7]	(190.6) [5.2]	(0.6) [4.1]	(44.9) [0.1]	(0.2) [747.4]
FX-2-7	60	14.0–15.0	8.3–8.6	302.4–319.0	5.0–7.2	22.2–25.8	170.8–213.5	0.4–0.6	40.7–65.6	− 1.6–1.3
		(14.5) [2.8]	(8.5) [1.1]	(312.4) [2.1]	(5.7) [15.3]	(23.8) [6.7]	(188.9) [8.3]	(0.5) [16.5]	(50.5) [0.2]	(− 0.3) [− 415.2]
FX-2-8	70	14.3–14.8	8.4–8.7	295.7–320.0	4.5–5.8	21.2–25.9	170.8–201.3	0.4–0.7	28.8–61.1	− 1.5–1.8
		(14.5) [1.3]	(8.6) [1.4]	(310.7) [3.0]	(5.3) [9.8]	(23.5) [8.3]	(186.1) [5.9]	(0.6) [17.3]	(43.6) [0.3]	(0.0) [− 121,027.4]
FX-2-9	80	14.4–14.9	8.3–8.6	299.8–322.0	3.9–6.2	22.2–26.1	176.9–213.5	0.4–0.6	37.2–76.0	− 1.7–1.9
		(14.6) [1.5]	(8.5) [1.4]	(311.7) [2.8]	(5.2) [16.8]	(24.0) [7.4]	(188.6) [7.7]	(0.5) [18.1]	(53.8) [0.3]	(0.1) [2808.8]
FX-2-10	90	14.3–15.0	8.2–8.6	304.5–323.0	3.6–6.1	21.7–26.8	176.9–195.2	0.3–0.7	36.6–85.5	− 1.7–2.1
		(14.6) [1.7]	(8.5) [1.7]	(313.1) [2.3]	(5.2) [18.9]	(24.1) [8.4]	(184.5) [3.6]	(0.5) [25.8]	(53.6) [0.4]	(0.1) [1103.4]
FX-2-11	100	14.0–14.8	8.4–8.6	300.8–319.0	4.4–6.3	22.1–26.3	170.8–195.2	0.5–0.7	36.7–57.2	− 1.4–1.7
		(14.5) [2.0]	(8.5) [0.9]	(311.6) [2.3]	(5.2) [12.9]	(24.0) [7.6]	(182.0) [5.0]	(0.5) [14.5]	(46.5) [0.2]	(0.0) [3705.7]
FX-2-12	110	14.2–14.6	8.3–8.5	303.1–322.0	3.7–5.5	21.9–27.4	176.9–219.6	0.4–0.5	46.0–83.4	− 1.9–2.1
		(14.4) [1.1]	(8.4) [1.2]	(313.0) [2.6]	(5.0) [15.5]	(24.2) [8.9]	(189.6) [9.3]	(0.5) [12.1]	(63.5) [0.3]	(− 0.1) [− 2397.5]
FX-3-1	0	15.1–22.9	8.5–9.0	287.3–318.0	7.7–9.5	19.4–25.4	176.9–201.3	0.6–1.0	13.6–46.0	− 1.0–1.4
		(18.8) [16.3]	(8.8) [2.2]	(304.3) [4.2]	(8.4) [8.5]	(22.5) [11.7]	(187.6) [4.8]	(0.9) [17.5]	(25.1) [0.5]	(0.3) [308.9]
FX-3-2	10	15.0–22.1	8.5–9.0	286.4–318.0	7.7–9.0	19.8–25.9	170.8–189.1	0.5–0.9	13.8–54.0	− 1.2–1.8
		(18.5) [15.4]	(8.8) [2.3]	(304.4) [4.3]	(8.3) [5.6]	(22.7) [12.4]	(181.5) [3.7]	(0.8) [19.9]	(28.5) [0.5]	(0.4) [281.7]
FX-3-3	20	15.0–20.9	8.5–9.0	286.5–318.0	7.0–8.8	19.9–26.0	176.9–195.2	0.6–0.9	14.7–51.8	− 1.1–1.4
		(18.0) [14.1]	(8.7) [2.1]	(306.4) [4.1]	(7.9) [8.4]	(23.2) [10.6]	(186.0) [3.7]	(0.8) [17.8]	(32.0) [0.4]	(0.3) [323.3]
FX-3-4	30	15.1–20.6	8.5–9.0	287.1–318.0	7.3–8.0	19.7–26.1	176.9–201.3	0.5–0.9	14.7–52.6	− 1.0–1.4
		(17.9) [13.7]	(8.7) [2.2]	(306.6) [4.1]	(7.7) [3.6]	(22.9) [11.4]	(186.0) [4.9]	(0.8) [18.8]	(31.6) [0.4]	(0.3) [336.3]
FX-3-5	40	15.0–20.2	8.5–8.8	296.2–318.0	6.6–7.7	20.5–25.8	183.0–207.4	0.6–0.8	23.9–50.1	− 1.1–1.8
		(17.6) [12.7]	(8.7) [1.4]	(309.5) [2.9]	(7.1) [4.5]	(23.2) [10.1]	(189.1) [5.6]	(0.7) [13.9]	(35.0) [0.3]	(0.2) [575.3]
FX–3–6	50	14.9–19.4	8.4–8.8	298.0–320.0	6.0–6.5	20.8–26.4	176.9–195.2	0.5–0.8	25.5–66.8	− 1.1–1.2
		(17.3) [11.7]	(8.6) [1.8]	(311.2) [2.8]	(6.5) [5.0]	(23.5) [10.0]	(184.5) [3.6]	(0.6) [18.9]	(41.8) [0.4]	(0.0) [− 11618.3]

[a]Minimum–maximum

[b]Mean values

[c]CV or variation coefficients = (standard deviation/mean)%

Cole et al. 1994). Cole et al. (1994) estimated that the mean partial pressure of CO_2 of lake water could be as high as three times that of the overlying atmosphere. However, our results showed that there existed both efflux and influx of CO_2 in Fuxian Lake during the study period (Table 2, Fig. 3). Furthermore, pCO_2 and DO followed opposite trends Fuxian Lake at different water depths of the water column over the year (Fig. 6), indicating that strong aquatic photosynthesis (with high DO concentration as an indicator) in lake waters might be an important carbon sink as this results in the absorption of CO_2 directly from the atmosphere, such as what occurs in the ocean (Passow and

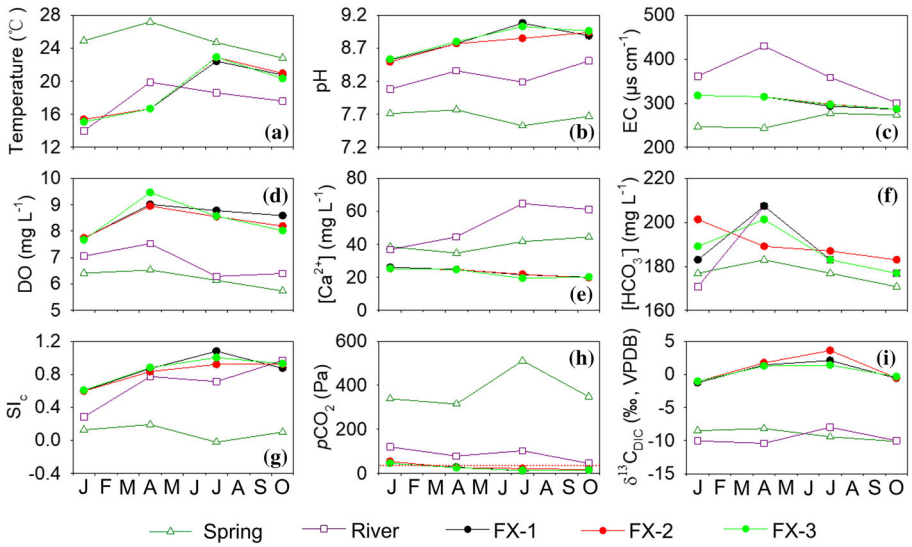

Fig. 2 A comparison of **a** temperature, **b** pH, **c** EC, **d** DO, **e** [Ca^{2+}], **f** [HCO_3^-], **g** SI_c, **h** pCO_2 and **i** $\delta^{13}C_{DIC}$ determined in 2017 in Luchong Spring, Liangwang River, and the surface water of Fuxian Lake (FX-1, FX-2, FX-3; water depth of 0.5 m). Dashed line represents CO_2 concentration in equilibrium with the atmosphere

Carlson 2012). In the euphotic zone, the photosynthesis of aquatic plants consumes CO_2 in the water and produces O_2. With increasing depth, light intensity decreases, and the photosynthetic metabolism of aquatic phototrophs weakens.

Stable carbon isotopic composition ($\delta^{13}C$) is usually used to constrain the carbon sources (Han et al. 2010; Cui et al. 2017). The main controls on the $\delta^{13}C_{DIC}$ in most lake waters are: (i) river and groundwater contributions; (ii) CO_2 exchanges of the water-atmosphere interface; (iii) carbonate mineral precipitation or dissolution reactions; (iv) CO_2 contributed by degradation of organic matter; and (v) photosynthetic utilization of ^{12}C into organic carbon (McKenzie 1985; Falkowski and Raven 1997; Xu et al. 2006; Lamb et al. 2007; Li et al. 2008; Chen et al. 2018). In this study, the $\delta^{13}C_{DIC}$ of spring and river waters in the Fuxian Lake basin had smaller coefficients of variation (spring, −8.5%; river, −9.9%; Table 1), which was in good agreement with the trend in the surface water of Fuxian Lake. However, this was unable to account for the relatively large variations of lake water (CV: −121,027.4%–3705.7%; Table 2). As already noted, higher pCO_2 (than atmospheric) and lower pH values, favoring chemically enhanced emission of CO_2 rather than influx, were observed in the surface waters during winter mixing in January. Theoretically, this would result in a higher $\delta^{13}C_{DIC}$, but this was contrary to the results observed by our monitoring. Furthermore, some studies have confirmed that lacustrine water with more negative $\delta^{13}C_{DIC}$ values reflected increased decomposition of organic matter (Wachniew and Różański 1997) and precipitation of carbonate minerals (Valero-Garcés et al. 1999). In the present study, however, the increasingly positive $\delta^{13}C$ values obtained from January to July (Fig. 5), when the decomposition of organic matter and the calcite deposition collected in the sediment traps both increased gradually, indicated that the relative importance of these two mechanisms could not be determined by direct observations. Indeed, the increasingly negative hypolimnetic values may partly be due to a weakening of photosynthesis and degradation of organic carbon, which produced the ^{13}C-depleted DIC (Parker et al. 2010).

Variations in $\delta^{13}C_{DIC}$ values are strongly associated with biological processes; for example, changes in the $^{13}C/^{12}C$ ratio are a response to algal productivity (McKenzie 1985; Chen et al. 2017). Over time, the increased biomass would assimilate proportionally larger amounts of ^{12}C, leaving the DIC pool enriched in ^{13}C. This concurs with the more positive $\delta^{13}C_{DIC}$ in the surface water in July and the heavier $\delta^{13}C_{DIC}$ in the epilimnion than in the hypolimnion (Fig. 5). This indicates how important the influence of aquatic photosynthesis is on the stable carbon isotopic compositions of DIC.

To better understand the concept of the mechanisms controlling the processes underpinning hydrochemistry in terrestrial aquatic ecosystems, atmospheric/soil CO_2 uptake was modeled by coupling carbonate weathering with an aquatic photosynthesis mechanism (CCW) (Liu et al. 2018), as follows:

$$\begin{aligned} &CaCO_3 + CO_2 + H_2O \rightarrow Ca^{2+} \\ &\quad + 2HCO_3^- \xrightarrow{\text{photosynth.}} CaCO_3 \\ &\quad + x(CO_2 + H_2O) + (1-x)(CH_2O + O_2) \end{aligned} \tag{6}$$

where x and 1-x are stoichiometric coefficients.

According to Eq (6), carbonate weathering coupled with aquatic photosynthesis (the biological carbon pump effect—"BCP") forms organic matter. This suggests that variations of hydrochemistry in the lake waters were

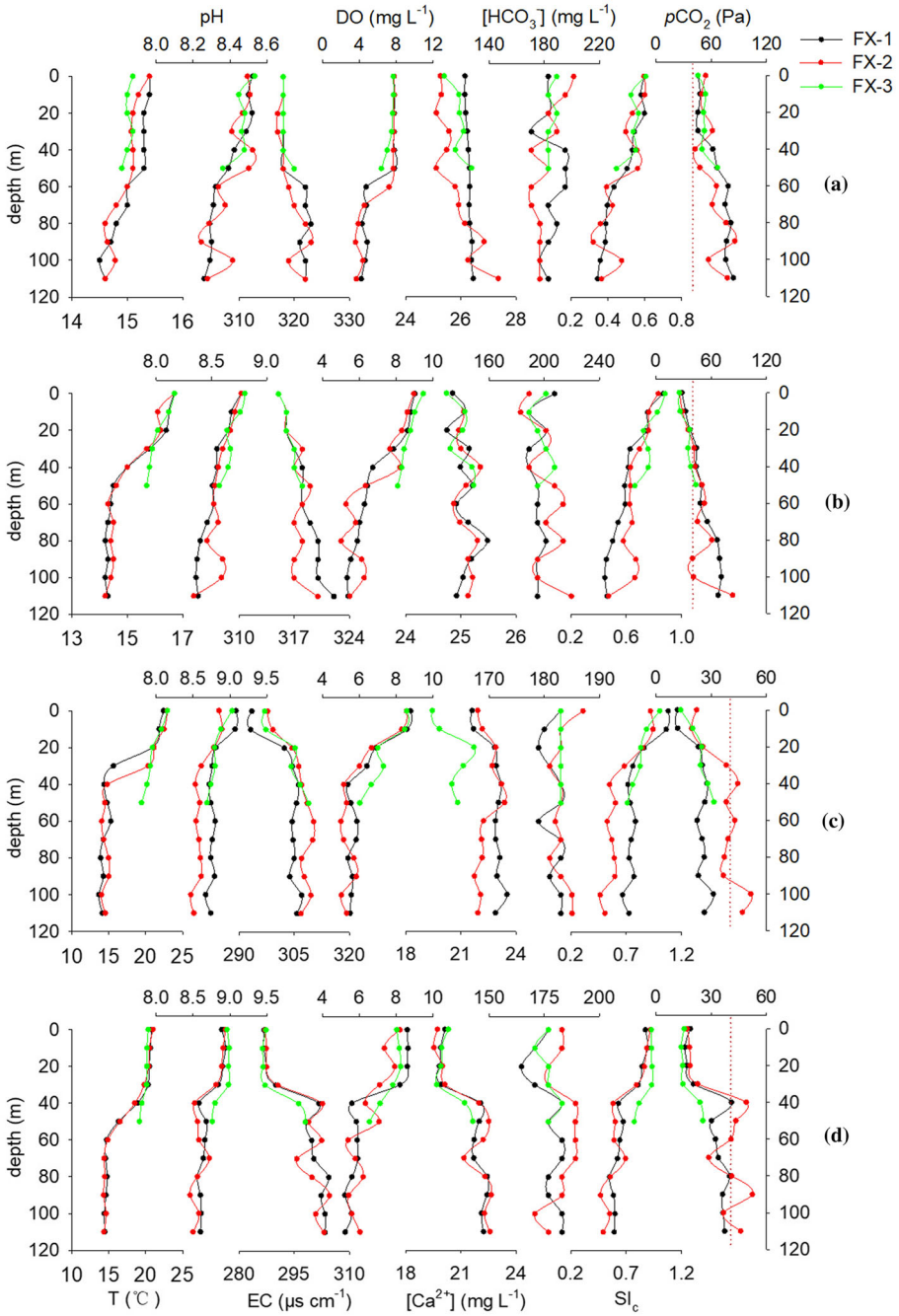

Fig. 3 Depth profiles of the physiochemical parameters monitored in winter (**a**), autumn (**b**), summer (**c**), and autumn (**d**) at sites FX-1, FX-2, and FX-3 in Fuxian Lake (1/2017–10/2017). The dashed line represents the CO_2 concentration in equilibrium with the atmosphere

mainly due to aquatic photosynthesis, and thus predominantly controlled by the BCP effect.

5.2 Sources of sedimentary organic matter in trap sediments of Fuxian Lake

The C/N ratios of organic matter can be used effectively to indicate the relative contribution of allochthonous versus autochthonous organic matter to lake sediment (Meyers and Ishiwatari 1993; Meyers 1997, 2003). Generally, C/N ratios for phytoplankton, soil, and terrigenous plants are 6.6 (Redfield 1963), 10–13 (Goñi et al. 2003), and 20 (Meyers 2003), respectively. In this study, the average value of C/N of lake sediment OC was 8.81 (Table 3); this is consistent with a composite of the three, with the aquatic plant proportion being predominant. $\delta^{13}C_{org}$ values may also be used to determine the relative contributions of autochthonous organic matter to lake sediment (Meyers and Ishiwatari 1993; Meyers 1997). Aquatic plants tend to have lighter $\delta^{13}C_{org}$ values due to the isotopic fractionation of aquatic photosynthesis (Falkowski and Raven 1997). As shown in Fig. 7, data from Fuxian Lake trap sediments

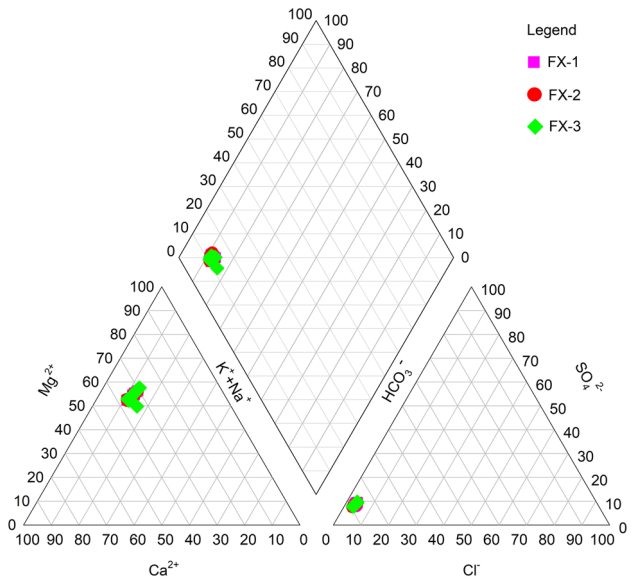

Fig. 4 Piper diagram of water samples from Fuxian Lake

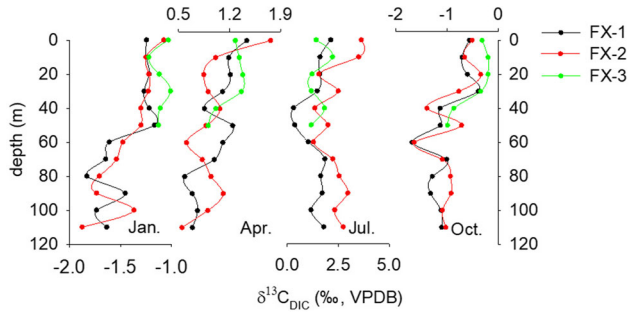

Fig. 5 A comparison of seasonal variations (1/2017–10/2017) in $\delta^{13}C_{DIC}$ at sites FX-1, FX-2 and FX-3 in Fuxian Lake

were within the range for autochthonous organic matter and were different from the range for allochthonous organic matter. In addition, there was a positive relationship between $\delta^{13}C_{org}$ and $\delta^{13}C_{carb}$ ($R^2 = 0.51$, $P < 0.05$, n = 9; Fig. 8) in this year-long study of trap sediments, suggesting both inorganic and organic carbon reflected variations in the isotopic composition of contemporaneous DIC (Meyer et al. 2013). This confirmed that organic matter in the Fuxian Lake sediments was chiefly derived from aquatic plants.

In the following, we quantitatively determine the proportions of the autochthonous and allochthonous organic matter in lake sediments by examining C/N ratios.

Terrigenous allochthonous C/N ratios were 12.71 (n = 6) using the average values of soil data in this watershed collected during this study and Ding et al. (2016), which were close to the experimental range of end element values (10–13) of soil organic carbon (Goñi et al. 2003). It is important to note that we regard soil as a typical allochthonous source because the direct input from terrestrial vegetation is relatively small. Liang et al. (2018) found that the C/N ratio of primary producers in ten lakes with different nutrient levels in Eastern Yunnan had low C/N ratios, with mean values of 7.68, slightly higher than the mean value of 6.69 from the present study of Fuxian Lake. Similarly, autochthonous the C/N ratio (7.02) was determined by the average value of these studies. Based on the Eq. (4), the proportions of autochthonous OC ranged from 30 to 100% (Table 4). The mean value of the proportions was 58% in trap sediments, which was comparable to that (61%) obtained in a recent study (Chen et al. 2018), indicating that lake OC was largely affected by the BCP effect.

Table 3 Dry weight, TOC and TIC contents, C/N ratios, $\delta^{13}C_{carb}$, $\delta^{13}C_{org}$, OCAR, ICAR and Total AR determined from sediment traps at site FX-2, Fuxian Lake, from different water depths in different seasons

Season	Water depth (m)	dry weight (g)	TOC (mg g^{-1})	TIC (mg g^{-1})	C/N	$\delta^{13}C_{carb}$ (‰)	$\delta^{13}C_{org}$ (‰)	OCAR (g C m^{-2} day^{-1})	ICAR (g C m^{-2} day^{-1})	Total AR (g C m^{-2} day^{-1})
Spring	40	0.71	106.57	3.22	9.44	− 1.31	− 26.98	0.047	0.001	0.442
	80	1.01	92.45	6.63	9.49	− 0.68	− 26.37	0.058	0.004	0.628
	110	1.13	107.78	9.14	8.60	− 1.40	− 27.27	0.076	0.006	0.703
Summer	40	1.61	76.48	72.82	9.30	− 0.35	− 24.63	0.077	0.073	1.001
	80	2.07	66.41	73.79	10.17	− 0.29	− 24.48	0.085	0.095	1.287
	110	1.87	80.97	63.54	10.18	− 0.16	− 25.37	0.094	0.074	1.163
Fall	80	4.74	45.20	80.87	6.65	0.01	− 20.88	0.133	0.238	2.947
Winter	40	0.77	102.24	18.39	7.06	− 0.85	− 23.89	0.049	0.009	0.479
	110	0.77	92.21	17.07	8.38	− 0.68	− 23.52	0.044	0.001	0.481

Table 4 The contribution percentages of autochthonous OC and allochthonous OC to the bulk OC in the sediment traps at site FX-2, Fuxian Lake, from different water depths in different seasons

Season	Water depth (m)	R_{auto} (%)	R_{allo} (%)	$OCAR_{auto}$ (g C m^{-2} day^{-1})	$ICAR_{allo}$ (g C m^{-2} day^{-1})
Spring	40	42.7	57.3	0.020	0.027
	80	41.9	58.1	0.024	0.034
	110	59.1	40.9	0.045	0.031
Summer	40	45.2	54.8	0.035	0.042
	80	30.9	69.1	0.026	0.059
	110	30.7	69.3	0.029	0.065
Fall	80	100.0	0.0	0.150	0.000
Winter	40	98.6	1.4	0.048	0.001
	110	63.8	36.2	0.028	0.016

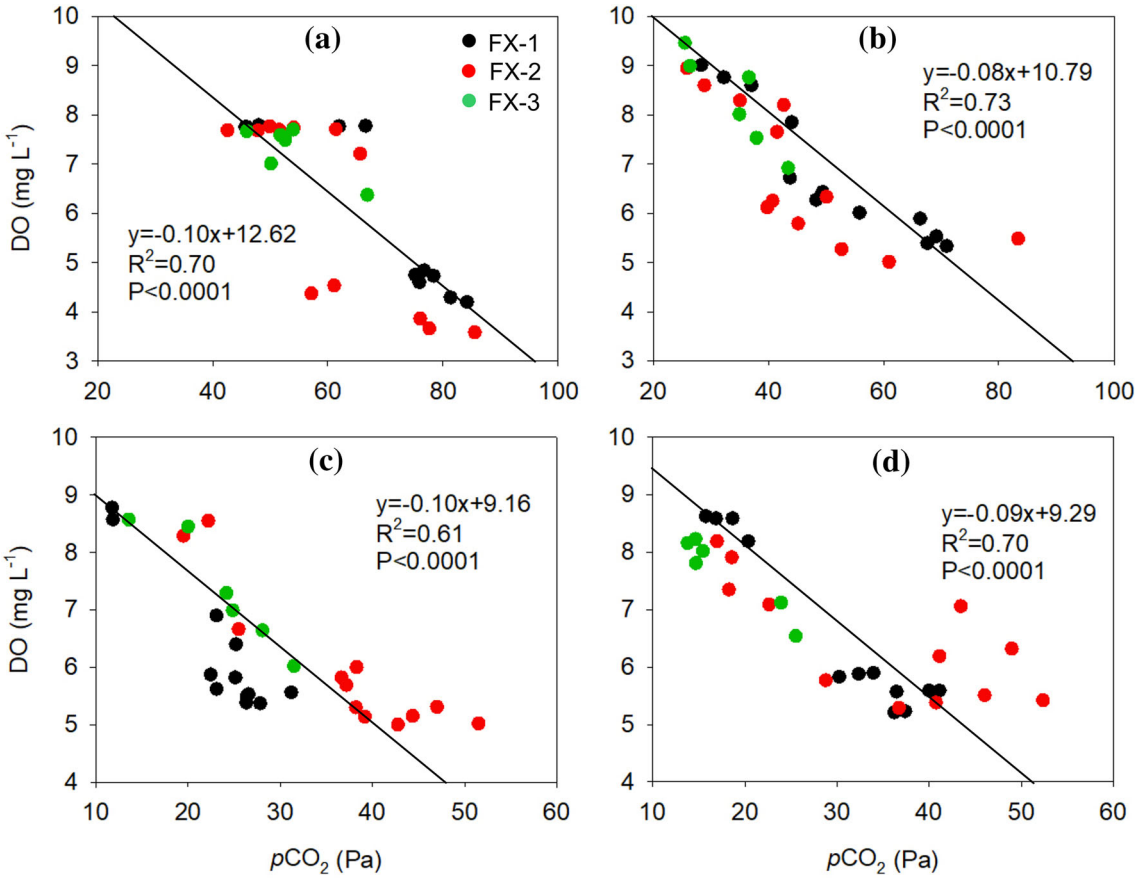

Fig. 6 Relationship between pCO_2 and DO in winter (**a**), autumn (**b**), summer(**c**) and autumn (**d**) at sites FX-1, FX-2 and FX-3 in Fuxian Lake

5.3 Autochthonous organic carbon sedimentation in the lake

5.3.1 Synchronous increase in $OCAR_{auto}$ and ICAR caused by the BCP effect

Fuxian Lake was saturated with calcite throughout the year and precipitated calcite in summer and fall in response to increases in pH caused by increased rates of aquatic photosynthesis. This increased organic productivity, due to the strong BCP effect, may cause greater precipitation of $CaCO_3$ (Kelts and Hsü 1978). According to Eq. (6), when the BCP effect occurs in aquatic ecosystems, there will be a synchronous increase in $OCAR_{auto}$ and ICAR. In the current study, the significant positive correlation between $OCAR_{auto}$ and ICAR in the trap sediments (R^2 = 0.69,

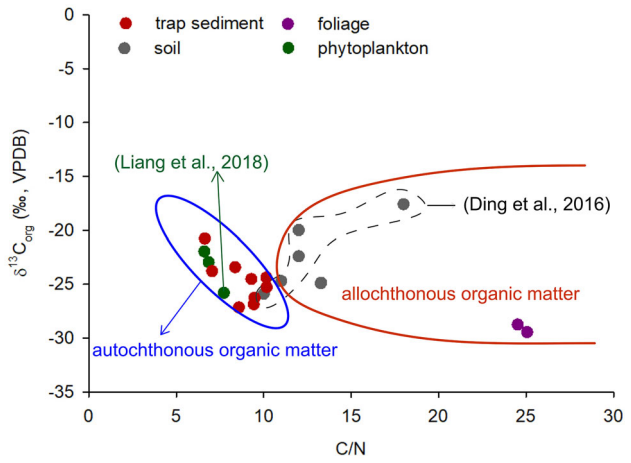

Fig. 7 Distinctive source combinations of C/N ratios and $\delta^{13}C_{org}$ values of the trap sediments, soil, foliage, and phytoplankton in Fuxian Lake

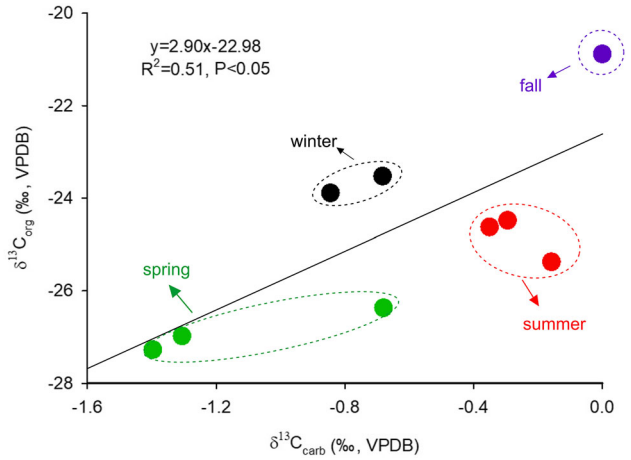

Fig. 8 Correlations between $\delta^{13}C_{org}$ and $\delta^{13}C_{carb}$ in the trap sediments during the monitoring year, 1/2017–1/2018

$P < 0.006$, n = 9; Fig. 9) illustrate this. However, the observed increase in $OCAR_{auto}$ with depth can be explained either by input from the euphotic zone, lateral input into the traps, or resuspension of OC, particularly in the very deep trap (Usbeck et al. 2003). This phenomenon can also be shown in ICAR. Therefore, we chose the upper trap (40 m) to conservatively calculate the $OCAR_{auto}$ as the actual autochthonous OC produced by the BCP effect, mainly to reduce the effect of resuspension. By that calculation, the AOC flux in the Fuxian Lake was 20.43 t C km^{-2} in 2017.

5.3.2 *Possible impacts of anthropogenic activities and climatic changes*

There is now a general agreement that the biogeochemical cycles of phosphorus and nitrogen have had considerable

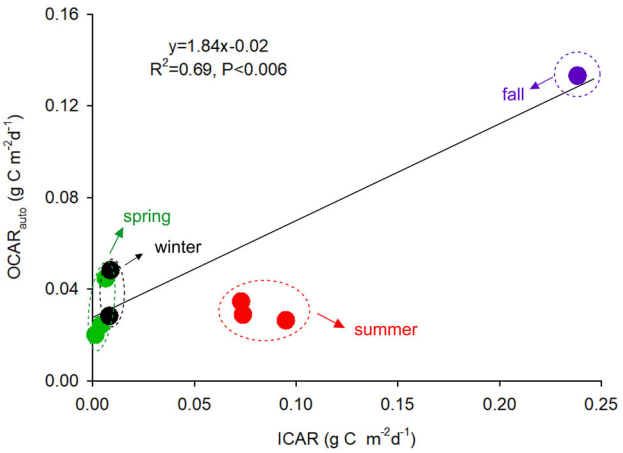

Fig. 9 Correlations between $OCAR_{auto}$ and ICAR in trap sediment during the monitoring period January 2017–January 2018

impacts on global lake productivity (Schindler et al. 1999). The increased $OCAR_{auto}$ from July to October may have been caused by increased river-borne nutrients and phosphorus inputs to the euphotic zone from the more than 20 short rivers across the basin of Fuxian Lake. Indeed, the concentrations of TP in the surface water were significantly higher in the wet season, which was mainly caused by pollutants contained in runoff (Yao et al. 2017). The temperature could be an alternative explanation for the high $OCAR_{auto}$ from July to October. The proportion of OC deposited (i.e., the burial efficiency) will increase with high temperatures due to enhanced aquatic photosynthesis (Lewis 2011; Brothers et al. 2008; Sobek et al. 2014), though warmer water temperatures can lead to mineralization and less organic carbon burial, as previously discussed (Gudasz et al. 2010).

6 Conclusions

By combining modern hydrochemical monitoring and a sediment trap experiment in Fuxian Lake (Yunnan, SW China), we conducted a systematic study to understand how much of the AOC was generated by the BCP effect can be deposited effectively and what the underlying mechanisms were. The main findings of this study were as follows:

1. Temperature, pH, EC (electric conductivity), DO (dissolved O_2), [HCO_3^-], [Ca^{2+}], SI_c, and partial pressures of CO_2 (pCO_2), as well as carbon isotopic compositions of HCO_3^- ($\delta^{13}C_{DIC}$) in Fuxian Lake water, all displayed distinct seasonal and vertical variations. This was especially apparent in an anti-correlation between pCO_2 and DO, indicating that the variations of hydrochemistry in lake waters were

mainly controlled by the photosynthetic metabolism of aquatic autotrophs.

2. The low C/N ratios and high $\delta^{13}C_{org}$ were recorded in the trap sediments. From observed C/N ratios, the proportions of AOC were estimated to be 30%–100% of all OC, indicating that AOC was an important contributor to sedimentary OC.
3. It was calculated that AOC flux in the Fuxian Lake was 20.43 t C km^{-2} in 2017, and this was affected by synergistic effects, including nutrient availability and climatic factors.
4. AOC formed by coupled carbonate weathering and aquatic photosynthesis (the BCP effect) may be a significant potential carbon sink and may make an important contribution to resolving the problem of the missing carbon sink in the global carbon cycle. If this process holds for all global lakes, the challenge would be to enhance carbon sequestration via the BCP effect.

Acknowledgements This work was supported by the National Natural Science Foundation of China (Nos. 41430753, U1612441).

References

Brenner M, Whitmore TJ, Curtis JH, Hodell DA, Schelske CL (1999) Stable isotope ($\delta^{13}C$ and $\delta^{15}N$) signatures of sedimented organic matter as indicators of historic lake trophic state. J Paleolimnol 22(2):205–221

Broecker WS, Takahashi T, Simpson HJ, Peng TH (1979) Fate of fossil fuel carbon dioxide and the global carbon budget. Science 206(4417):409–418

Brothers S, Vermaire JC, Gregory-Eaves I (2008) Empirical models for describing recent sedimentation rates in lakes distributed across broad spatial scales. J Paleolimnol 40(4):1003–1019

Chen B, Yang R, Liu ZH, Sun HL, Yan H, Zeng QR, Zeng SB, Zeng C, Zhao M (2017) Coupled control of land uses and aquatic biological processes on the diurnal hydrochemical variations in the five ponds at the Shawan Karst Test Site, China: implications for the carbonate weathering-related carbon sink. Chem Geol 456:58–71

Chen JA, Yang HQ, Zeng Y, Guo JY, Song YL, Ding W (2018) Combined use of radiocarbon and stable carbon isotope to constrain the sources and cycling of particulate organic carbon in a large freshwater lake, China. Sci Total Environ 625:27–38

Ciais P et al (2013) Carbon and other biogeochemical cycles. In: Stocker TF (ed) Climate Change 2013: The physical science basis. Contribution of working group I to the fifth assessment report of the intergovernmental panel on climate change. Cambridge University Press, Cambridge, pp 465–570

Cole JJ, Caraco NF, Kling GW, Kratz TK (1994) Carbon dioxide supersaturation in the surface waters of lakes. Science 265(5178):1568–1570

Cole JJ, Prairie YT, Caraco NF, McDowell WH, Tranvik LJ, Striegl RG, Melack J (2007) Plumbing the global carbon cycle: integrating inland waters into the terrestrial carbon budget. Ecosystems 10(1):172–185

Cui GY, Li XD, Li QK, Huang J, Tao YL, Li SQ, Zhang J (2017) Damming effects on dissolved inorganic carbon in different kinds of reservoirs in Jialing River, Southwest China. Acta Geochim 36(4):581–597

Ding W, Chen JA, Yang HQ, Tao HB, Luo J (2016) Investigation on sources of organic carbon in major rivers in the catchment of Fuxian Lake, Yunnan Province. Earth Environ 44(3):290–296

Falkowski PG, Raven JA (1997) Aquatic photosynthesis. Blackwell Science, Oxford

Galy V, Eglinton T, France-Lanord C, Sylva S (2011) The provenance of vegetation and environmental signatures encoded in vascular plant biomarkers carried by the Ganges–Brahmaputra rivers. Earth Planet Sci Lett 304(1–2):1–12

Goñi MA, Teixeira MJ, Perkey DW (2003) Sources and distribution of organic matter in a river-dominated estuary (Winyah Bay, SC, USA). Estuar Coast Shelf Sci 57(5–6):1023–1048

Gudasz C, Bastviken D, Steger K, Premke K, Sobek S, Tranvik LJ (2010) Temperature-controlled organic carbon mineralization in lake sediments. Nature 466(7305):478

Han GL, Tang Y, Wu QX (2010) Hydrogeochemistry and dissolved inorganic carbon isotopic composition on karst groundwater in Maolan, Southwest China. Environ Earth Sci 60(4):893–899

Hollander DJ, McKenzie JA (1991) CO_2 control on carbon-isotope fractionation during aqueous photosynthesis: a paleo-pCO_2 barometer. Geology 19(9):929–932

Huang CC, Yao L, Zhang YL, Huang T, Zhang ML, Zhu AX, Yang H (2017) Spatial and temporal variation in autochthonous and allochthonous contributors to increased organic carbon and nitrogen burial in a plateau lake. Sci Total Environ 603:390–400

Kelts K, Hsü KJ (1978) Freshwater carbonate sedimentation. In: Lakes. Springer, New York, pp 295–323

Lamb HF, Leng MJ, Telford RJ, Ayenew T, Umer M (2007) Oxygen and carbon isotope composition of authigenic carbonate from an Ethiopian lake: a climate record of the last 2000 years. Holocene 17(4):517–526

Lewis WM Jr (2011) Global primary production of lakes: 19th Baldi Memorial Lecture. Inland Waters 1(1):1–28

Li SL, Liu CQ, Lang YC, Tao F, Zhao ZQ, Zhou ZH (2008) Stable carbon isotope biogeochemistry and anthropogenic impacts on karst ground water, Zunyi, Southwest China. Aquat Geochem 14(3):211

Liang H, Huang LP, Chen GJ, Kang WG, Liu YY, Wang JY, Zhu QS, Liu S, Deng Y (2018) Patterns of carbon and nitrogen stable isotopes and elemental composition of lake primary producers and zooplankton in Eastern Yunnan. J Lake Sci 30(5):1400–1412

Liu ZH, Dreybrod W (1997) Dissolution kinetics of calcium carbonate minerals in H_2O–CO_2 solutions in turbulent flow: the role of the diffusion boundary layer and the slow reaction $H_2O + CO_2 \rightarrow H^+ + HCO_3^-$. Geochim Cosmochim Acta 61(14):2879–2889

Liu Y, Wu G, Gao ZW (2008) Impacts of land-use change in Fuxian and Qilu basins of Yunnan Province on lake water quality. Chin J Ecol 27(3):447–453

Liu ZH, Dreybrodt W, Wang HJ (2010) A new direction in effective accounting for the atmospheric CO_2 budget: considering the combined action of carbonate dissolution, the global water cycle and photosynthetic uptake of DIC by aquatic organisms. Earth Sci Rev 99(3–4):162–172

Liu ZH, Dreybrodt W, Liu H (2011) Atmospheric CO_2 sink: silicate weathering or carbonate weathering? Appl Geochem 26:S292–S294

Liu ZH, Macpherson GL, Groves C, Martin JB, Yuan DX, Zeng SB (2018) Large and active CO_2 uptake by coupled carbonate weathering. Earth Sci Rev 182:42–49

McKenzie JA (1985) Carbon isotopes and productivity in the lacustrine and marine environment. In: Stumm W (ed) Chemical processes in lakes. Wiley, New York, pp 99–118

Melnikov NB, O'Neill BC (2006) Learning about the carbon cycle from global budget data. Geophys Res Lett 33(2)

Meyer KM, Yu M, Lehrmann D, Van de Schootbrugge B, Payne JL (2013) Constraints on early triassic carbon cycle dynamics from paired organic and inorganic carbon isotope records. Earth Planet Sci Lett 361:429–435

Meyers PA (1997) Organic geochemical proxies of paleoceanographic, paleolimnologic, and paleoclimatic processes. Org Geochem 27(5–6):213–250

Meyers PA (2003) Applications of organic geochemistry to paleolimnological reconstructions: a summary of examples from the Laurentian Great Lakes. Org Geochem 34(2):261–289

Meyers PA, Ishiwatari R (1993) Lacustrine organic geochemistry: an overview of indicators of organic matter sources and diagenesis in lake sediments. Org Geochem 20(7):867–900

O'Reilly SS, Szpak MT, Flanagan PV, Monteys X, Murphy BT, Jordan SF, Kelleher BP (2014) Biomarkers reveal the effects of hydrography on the sources and fate of marine and terrestrial organic matter in the western Irish Sea. Estuar Coast Shelf Sci 136:157–171

Parker SR, Gammons CH, Poulson SR, DeGrandpre MD, Weyer CL, Smith MG, Oba Y (2010) Diel behavior of stable isotopes of dissolved oxygen and dissolved inorganic carbon in rivers over a range of trophic conditions, and in a mesocosm experiment. Chem Geol 269(1–2):22–32

Parkhurst DL, Appelo CAJ (1999) User's guide to PHREEQC (version 2): a computer program for speciation, batch-reaction, one-dimensional transport, and inverse geochemical calculations. In: US Geological Survey Water Resources Investigations Report, pp 99–4259

Passow U, Carlson CA (2012) The biological pump in a high CO_2 world. Mar Ecol Prog Ser 470:249–271

Ramaswamy V, Gaye B, Shirodkar PV, Rao PS, Chivas AR, Wheeler D, Thwin S (2008) Distribution and sources of organic carbon, nitrogen and their isotopic signatures in sediments from the Ayeyarwady (Irrawaddy) continental shelf, northern Andaman Sea. Mar Chem 111(3–4):137–150

Redfield AC (1963) The influence of organisms on the composition of seawater. Sea 2:26–77

Schindler DW (1999) Carbon cycling: the mysterious missing sink. Nature 398(6723):105

Sobek S, Tranvik LJ, Cole JJ (2005) Temperature independence of carbon dioxide supersaturation in global lakes. Glob Biogeochem Cycles 19(2)

Sobek S, Anderson NJ, Bernasconi SM, Del Sontro T (2014) Low organic carbon burial efficiency in arctic lake sediments. J Geophys Res: Biogeosci 119(6):1231–1243

Sun HG, Han JT, Zhang SR, Lu XX (2011) Transformation of dissolved inorganic carbon (DIC) into particulate organic carbon (POC) in the lower Xijiang River, SE China: an isotopic approach. Biogeosci Discus 8(5):9471–9501

Sundquist ET (1993) The global carbon dioxide budget. Science 934–941

Tue NT, Hamaoka H, Sogabe A, Quy TD, Nhuan MT, Omori K (2011) The application of $\delta^{13}C$ and C/N ratios as indicators of organic carbon sources and paleoenvironmental change of the mangrove ecosystem from Ba Lat Estuary, Red River, Vietnam. Environ Earth Sci 64(5):1475–1486

Usbeck R, Schlitzer R, Fischer G, Wefer G (2003) Particle fluxes in the ocean: comparison of sediment trap data with results from inverse modeling. J Mar Syst 39(3–4):167–183

Valero-Garcés BL, Delgado-Huertas A, Ratto N, Navas A (1999) Large ^{13}C enrichment in primary carbonates from Andean Altiplano lakes, northwest Argentina. Earth Planet Sci Lett 171(2):253–266

Wachniew P, Różański K (1997) Carbon budget of a mid-latitude, groundwater-controlled lake: isotopic evidence for the importance of dissolved inorganic carbon recycling. Geochim Cosmochim Acta 61(12):2453–2465

Wang SM, Dou HS (1998) China lakes chorography. Science Press, Beijing

Waterson EJ, Canuel EA (2008) Sources of sedimentary organic matter in the Mississippi River and adjacent Gulf of Mexico as revealed by lipid biomarker and $\delta^{13}C_{TOC}$ analyses. Org Geochem 39(4):422–439

Xiao HY (2017) Effects and underlying mechanisms of damming on carbon and nitrogen cycles and transport in rivers of southwest China: project introduction. Acta Geochim 36(4):577–580

Xu H, Ai L, Tan LC, An ZS (2006) Stable isotopes in bulk carbonates and organic matter in recent sediments of Lake Qinghai and their climatic implications. Chem Geol 235(3–4):262–275

Yao B, Liu QQ, Hu CM, Xi BD, Wu XH (2017) Distribution characteristics of phosphorus in the water of Lake Fuxian and its influencing factors. Sci Technol Rev 35(3):66–71